Determination of Absolute Recurrent Fluorescence Rate Coefficients for C 6 −

ARTICLE *in* JOURNAL OF PHYSICAL CHEMISTRY LETTERS · DECEMBER 2014

Impact Factor: 7.46 · DOI: 10.1021/jz502100z

9 AUTHORS, INCLUDING:

Bhim Prasad Kafle
Kathmandu University
20 PUBLICATIONS **77** CITATIONS
SEE PROFILE

Aneesh Prabhakaran
Thermo Fisher Scientific, Bremen
13 PUBLICATIONS **43** CITATIONS
SEE PROFILE

Oded Heber
Weizmann Institute of Science
173 PUBLICATIONS **2,202** CITATIONS
SEE PROFILE

Yoni Toker
Bar Ilan University
39 PUBLICATIONS **240** CITATIONS
SEE PROFILE

THE JOURNAL OF PHYSICAL CHEMISTRY Letters

Letter

pubs.acs.org/JPCL

Determination of Absolute Recurrent Fluorescence Rate Coefficients for C_6^-

Vijayanand Chandrasekaran,*[,†] Bhim Kafle,[†] Aneesh Prabhakaran,[†] Oded Heber,[†] Michael Rappaport,[†] Hilel Rubinstein,[†] Dirk Schwalm,[†,‡] Yoni Toker,[†] and Daniel Zajfman[†]

[†]Department of Particle Physics and Astrophysics, Weizmann Institute of Science, Rehovot, 76100, Israel

[‡]Max-Planck-Institut für Kernphysik, D-69117 Heidelberg, Germany

ABSTRACT: We determined absolute rate coefficients for the recurrent fluorescence (RF) process in C_6^- anions at excitation energies above the adiabatic electron attachment energy of 4.18 eV. The experiment was performed by extracting C_6^- ions from a sputter ion source and storing them in a bent electrostatic ion beam trap. After 1 s of storage, during which the anions cooled down to temperatures close to room temperature, they were excited by a short laser pulse and the neutralization rate due to vibrational autodetachment (VAD) was measured as a function of time at several wavelengths. Due to the different energy dependence of the two competing decays via the RF and the VAD process, their contributions to the measured total decay rate coefficients could be disentangled. For excitation energies $\lesssim$4.6 eV, the decay is found to be dominated by the RF process with decay rate coefficients on the order of 5×10^4 s^{-1}. The result clearly demonstrates the presence of the RF process in C_6^- and illustrates the importance of this process in the production and cooling of isolated molecules of astrophysical interest.

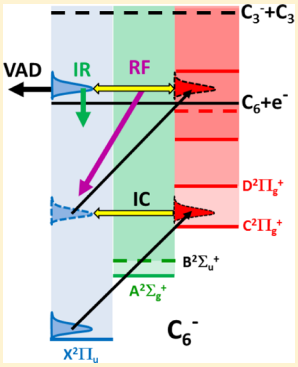

SECTION: Spectroscopy, Photochemistry, and Excited States

In the interstellar medium, carbonaceous molecules or dust particles are thought to be the carriers of unidentified infrared emission bands and diffuse interstellar absorption bands.[1] Until today, however, not a single carrier molecule has been identified unambiguously, which is an enduring motivation to study the photophysics of these molecules in the gas phase under conditions similar to the conditions present in space.

When a polyatomic molecule is excited by a photon from its electronic ground state to an excited electronic state, the excitation energy will usually be rapidly converted into vibrational energy due to nonadiabatic coupling between the electronically excited state and the vibrational quasi-continuum built on the electronic ground state, a process known as internal conversion (IC).[2] The reverse process, inverse internal conversion, and the emission of an optical photon, a process referred to as recurrent fluorescence (RF),[3] is expected to occur on considerably longer time scales due to the small statistical weight of the excited electronic state. However, in an collision-free environment, RF might very well compete with other decay channels such as fragmentation, electron emission via vibrational autodetachment (VAD),[4] or infrared (IR) transitions. The recurrent fluorescence process is therefore a critical ingredient for understanding the formation of molecules in space, where two-body reactions and UV absorption produce highly excited molecules, and radiative transitions determine their survival probability, and for understanding their electromagnetic emission spectra.

Despite the obvious importance of the RF process for the stabilization and cooling of interstellar molecules, and despite the advent of small storage devices that can provide the collision-free environment required for these studies, quantitative experimental information concerning the RF rates of these molecules is still sparse. The mechanism underlying recurrent fluorescence was originally discussed in connection with the luminescence observed in the chromyl chloride molecule after multiphoton excitation with IR photons.[5,6] Although IR-induced luminescence was observed in other molecules as well,[7] quantitative studies of the RF rates in these molecules were hampered by the occurrence of excited fragments and the inability of knowing the exact amount of absorbed energy. The first conclusive experimental evidence for the importance of this cooling mechanism in small polycyclic aromatic hydrocarbon molecules was obtained only recently by Martin et al.[8] Using an electrostatic Mini-ring,[9] they followed the evolution of the internal energy distribution of stored anthracene cations ($C_{14}H_{10}^+$) via laser excitation. For internal excitation energies around 6.7 eV, they deduced a radiative cooling rate of $\approx 2 \times 10^2$ s^{-1}, which is 2 orders of magnitude larger than the expected IR cooling rate, but consistent with the estimated emission rate involving the first excited electronic state of anthracene. More recently, Ito et al.[10] compared the cooling dynamics of C_6^- and C_6H^- by studying laser-induced electron detachment using the TMU E-ring.[11] While the decay times of C_6H^- were observed to be in the millisecond range, those of C_6^- were found to be shorter than 100 μs, in fact too short to be measured more precisely in their setup. The fast decay times are attributed to

Received: October 2, 2014
Accepted: November 10, 2014
Published: November 10, 2014

the presence of RF in C_6^-, while in the closed shell anion C_6H^- this decay channel is not available due to the lack of low-lying electronic states. In fact, the RF-mediated decay time in C_6^- was estimated in ref 12 to be around 35 μs.

In the present work we determined absolute RF rate coefficients for C_6^- anions using a bent electrostatic ion beam trap.[13] The low background pressure of $\approx 5 \times 10^{-11}$ mbar allowed us to cool the stored ions for 1 s before exciting them by a short laser pulse to energies above the adiabatic electron attachment energy of 4.18 eV,[14] and to follow their decay as a function of time over 4 orders of magnitude by measuring the neutralization rate due to vibrational autodetachment. This rate was found to show a nearly exponential time dependence, and the two competing decay channels contributing to the total decay rate coefficient, vibrational autodetachment, and radiative stabilization via recurrent fluorescence could be disentangled due to their different excitation energy dependence.

The experimental setup is shown in Figure 1. C_n^- clusters were produced in a Cs sputter source using a graphite target.

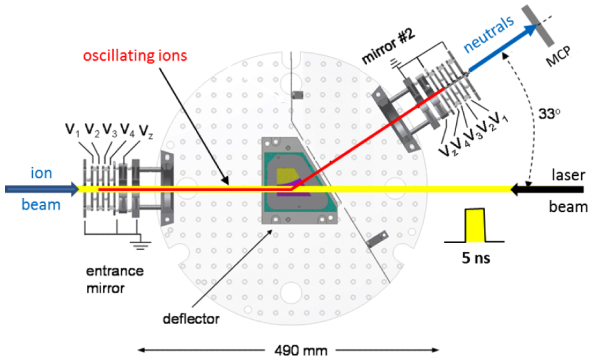

Figure 1. Bent electrostatic ion beam trap.[13]

After being bunched and accelerated to kinetic energies of 4.2 keV, the C_6^- ions were mass selected by a magnet (resolving power 1000:1) and then injected into a bent electrostatic ion beam trap (EIBT). After closing the trap, about 10^4 to 10^5 ions were trapped and oscillated back and forth between the two trap mirrors on a V-shaped trajectory with an oscillation period of 13.0 μs. After 1 s of storage, the C_6^- ions located between the entrance mirror and the electrostatic deflector were overlapped with a 5 ns-wide laser pulse with an average pulse energy of 0.5−1.0 mJ. UV and visible photons were used to excite the ions by a one- or two-photon process, respectively. While neutral products resulting from prompt electron detachment or fragmentation left the trap undetected, products from C_6^- ions neutralizing while traveling between the deflector and trap mirror #2 could be detected in the microchannel plate detector (MCP) located behind mirror #2. Thus, the experiment is sensitive only to delayed neutralization processes; the shortest decay time contributing to the detected signal is the transient time of the ions through the deflector, about 0.4 μs.

Examples of neutralization rates $R(t)$ observed after two-photon excitation of C_6^- at wavelengths of λ = 550, 580, and 615 nm are shown in Figure 2; the results were obtained by summing over ≈3000 injections. The observed decay curves are close to exponential, and corresponding fits with $R(t) \propto \exp(-k_\lambda t)$ for $t \geq 16.5$ μs (dashed red lines in Figure 2) result in effective decay times k_λ^{-1} of 10−20 μs. The first bin was excluded from the fit because the measured rate is expected to be reduced by dead time effects of the MCP at increasing

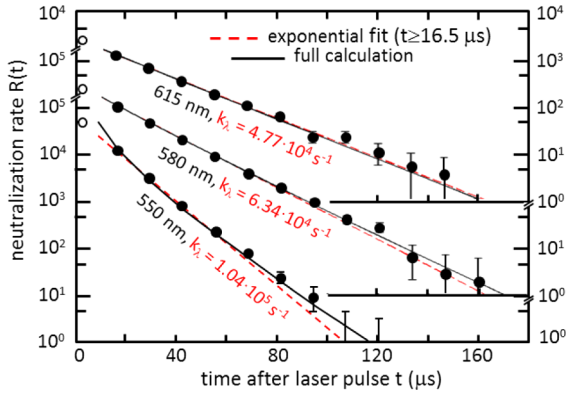

Figure 2. Neutralization rates observed as a function of time after two-photon excitation of C_6^- with a short laser pulse at three wavelengths. The laser was fired 1 s after the injection of the ions into the trap. The data (solid dots) were binned to 13.0 μs corresponding to one oscillation. The neutralization rate due to residual gas scattering, as determined from the event rate observed just before the laser pulse, has been subtracted.

photon energies due to the strongly increasing event rate. Note that the decay of the laser-excited anions can be followed over almost 10 decay times due to the high excitation and detection efficiency of our setup and the low background rate due to the excellent vacuum. The effective decay constants k_λ deduced after one- and two-photon excitation are plotted in Figure 3 as a function of the respective average total excitation energies $\hat{E}_\lambda$ of C_6^-, which are determined as discussed below.

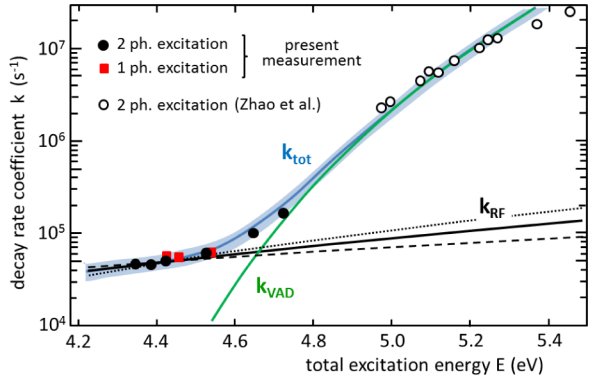

Figure 3. Experimental decay rate coefficients k_λ for C_6^- plotted as a function of the total excitation energy $E = \hat{E}_\lambda(t_0)$ (filled symbols: present experiment; unfilled circles: ref 23; statistical errors are smaller than the symbol size). The blue curve is the sum of the partial decay rate coefficients for vibrational autodetachment ($k_{VAD}(E)$, green line) and recurrent fluorescence ($k_{RF}(E)$, black line) given by eqs 1 and 2 and adjusted to the data by setting $F_{VAD} = 4.3 \times 10^{14} s^{-1}$ and $A_j = 1.67$ A_j^{th}, respectively. The thin lines show the $k_{RF}(E)$ coefficients for two extreme assumptions, viz., $A_1 = 0$, $A_2 = 3.7A_2^{th}$ (dotted) and $A_1 = 3.0$ A_1^{th}, $A_2 = 0$ (dashed).

For deriving $\hat{E}_\lambda$ and interpreting the deduced effective decay rate constants k_λ in terms of the contributing decay channels, we take advantage of the fact that the structure of the C_6^- anions has already been the subject of detailed experimental and theoretical studies.[14−25] The main properties of C_6^- relevant for the present study are summarized in Figure 4. After being stored for 1 s, the initially hot C_6^- anions are expected to be cooled down and to populate a narrow band of vibrational states built on the $^2\Pi_u$ ground state. Besides the $^2\Pi_u$ ground

dx.doi.org/10.1021/jz502100z | J. Phys. Chem. Lett. 2014, 5, 4078−4082

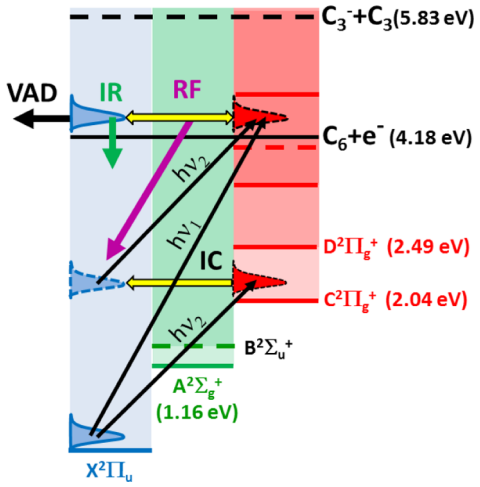

Figure 4. Summary of the main properties of C_6^- relevant for the present investigation, which concentrates on the competition between RF, VAD, and IR decays of states at excitation energies up to ~1 eV above the adiabatic electron attachment energy of 4.18 eV. At these energies, the dissociation channels are still closed, as the lowest fragmentation threshold is at 5.83 eV.[22] Possible one- and two-photon excitation paths involving internal conversion (IC) are indicated.

state and its fundamental vibrational excitation spectrum,[15,20,21] several excited electronic configurations of $^2\Sigma_g$ and $^2\Pi_g$ symmetry are experimentally known[16,17,23] or predicted[15,18,19] below the adiabatic electron attachment energy, which serve as doorway states for effective laser-excitation pathways and for the recurrent fluorescence process (Also quartet states are expected below the electron attachment energy, the lowest one being the $X^4\Pi_g$ state at E = 2.5 eV.[18] We shall ignore the quartet configurations: although quartet states are accessible when attaching an electron to $C_6(^3\Sigma_g)$, and these states might even remain in the quartet manifold after 1 s of cooling, their decay after excitation, even by a single photon, will be very fast and outside of the time window of our experiment). Laser excitation by one- and two-photon absorption to energies above the adiabatic electron attachment energy (EA) and the ultrafast IC process has been investigated in detail by the Neumark group.[23−25] We shall use this information to describe the excitation energy dependences of the partial decay constants, needed to estimate the internal energy distribution of C_6^- before laser excitation and to determine the excitation energy dependence of the neutralization rate, within the statistical rate theory.[26]

Based on the detailed balance approach, the energy dependence of the VAD rate coefficients $k_{\mathrm{VAD}}(E)$ can be approximated by

$$k_{\mathrm{VAD}}(E) = F_{\mathrm{VAD}} \int_0^{E-\mathrm{EA}} \sqrt{\epsilon}\, \frac{\rho_{C_6}(E - \mathrm{EA} - \epsilon)}{\rho_{C_6^-}(E)} d\epsilon \tag{1}$$

which makes the usual assumption that the electron capture cross section as a function of electron energy ϵ is given by the Langevin cross section[27] and is thus proportional to $\epsilon^{-1/2}$. ρ_{C_6} and $\rho_{C_6^-}$ are the vibrational level densities built on the electronic ground states of C_6 and C_6^-, respectively; they are calculated in the harmonic oscillator approach[28] using the respective (scaled) fundamental vibrational frequencies given in refs.[20,29] Contributions of higher-lying electronic configurations to the level densities are small and neglected. The absolute scale of $k_{\mathrm{VAD}}(E)$ is set by F_{VAD}, which is determined by adjusting eq 1 to the VAD rate coefficients measured in ref 23. This results in F_{VAD} = 4.3×10^{14} s^{-1} (see below).

The energy dependence of the RF rate coefficients $k_{\mathrm{RF},j}(E)$ is given by[30]

$$k_{\mathrm{RF},j}(E) = A_j(E_j) \frac{\rho_{C_6^-}(E - E_j)}{\rho_{C_6^-}(E)} \tag{2}$$

where $A_j(E_j)$ denotes the Einstein coefficient for the transition from the excited electronic state j to the ground state, and E_j is the energy difference between the band heads. Based on calculated oscillator strengths,[18,19] the RF process is expected to be dominated by the $A^2\Sigma_g$ state ($A_1^{\mathrm{th}}(1.16\ \mathrm{eV}) = 3.8 \times 10^5$ s^{-1}),[18] and the $C^2\Pi_g$ state ($A_2^{\mathrm{th}}(2.04\ \mathrm{eV}) = 6.7 \times 10^6$ s^{-1}).[19] In ref 18, the calculated oscillator strengths from the $X^2\Pi_u$ ground state to the $C^2\Pi_g$ state is a factor of ≈100 larger than the transition to the $X^2\Sigma_g$ state, and a factor of >10 larger than for other dipole allowed transitions, which is difficult to reconcile with observations.[17] We therefore adopted the 10 times smaller value calculated by Gao et al.[19] for the $C^2\Pi_g$ strength. Finally, the IR rate coefficients $k_{\mathrm{IR},\mu}(E)$ can be estimated using the harmonic oscillator approach, which results in[31]

$$k_{\mathrm{IR},\mu}(E) = \mathcal{A}_\mu(\hbar\omega_\mu) \sum_\kappa \frac{\rho_{C_6^-}(E - \kappa\hbar\omega_\mu)}{\rho_{C_6^-}(E)} \tag{3}$$

where the sum runs over the vibrational quantum numbers κ with $\kappa \geq 1$ and $(E - \kappa\hbar\omega_\mu) \geq 0$. The frequencies ω_μ of the 13 fundamental modes μ and the Einstein coefficients $\mathcal{A}_\mu(\hbar\omega_\mu)$ for the $\kappa = 1$ to $\kappa = 0$ transition are taken from theory.[20] The IR transitions are dominated by the asymmetric stretch mode (μ = 4) with $\hbar\omega_4$ = 0.24 meV and $\mathcal{A}_4^{\mathrm{th}}(0.24\ \mathrm{eV}) = 7.9 \times 10^2$ s^{-1}, while for the other infrared active transitions $\mathcal{A}_\mu^{\mathrm{th}} < 1$ s^{-1}.

Using eqs 1−3 we can now calculate the delayed neutralization rate $R(t)$ expected after excitation of cold C_6^- anions by a short laser pulse. As only excited states well below the lowest fragmentation threshold live long enough to contribute to the delayed signal, the neutralization rate is solely due to the VAD process. Moreover, cascade feeding of states above EA can be neglected as IR-mediated decays cannot compete with the RF process, and the latter involves transition energies >1 eV leading directly to states below EA. Denoting the internal energy distribution of the C_6^- ions after 1 s of storage by $f_0(E_i)$, the neutralization rate after the absorption of n photons of energy hc/λ is thus given by

$$R(t) = N \int_{\mathrm{EA}}^{\infty} f_0(E = E_i + nhc/\lambda) k_{\mathrm{VAD}}(E) e^{-k_{\mathrm{tot}}(E)t}\, \mathrm{d}E \tag{4}$$

assuming a constant photon crosssection over the width of $f_0(E_i)$. As discussed, for $E \geq$ EA the total decay rate coefficient $k_{\mathrm{tot}}(E)$, being the sum over all decay constants, is dominated by $k_{\mathrm{VAD}}(E)$ and $k_{\mathrm{RF}}(E) = \sum_{j=1,2} k_{\mathrm{RF},j}(E)$.

Equations 1−3 were also used together with the master equation approach to investigate the cooling of the initially hot C_6^- ions as a function of storage time t_s, and to estimate the internal energy distribution $f_0(E_i)$ to be expected after 1 s of storage. After the very fast cooling via the RF process (see also Ito et al.[10]), the further cooling up until ≈1 s is mainly controlled by the μ = 4 IR mode. For energies $E_i \lesssim 0.4$ eV, however, the level density $\rho_{C_6^-}(E - \hbar\omega_4)$ is getting too small for

dx.doi.org/10.1021/jz502100z | J. Phys. Chem. Lett. 2014, 5, 4078−4082

the statistical description to be valid. Indeed, at these energies the statistical approach is found to overestimate the cooling; as will be discussed in detail in a forthcoming publication, we followed the cooling experimentally and derived a modified $k_{IR}(E)$ rate, which results after t_s = 1 s in an approximately bell-shaped $f_0(E_i)$ distribution centered around ≈0.2 eV and with a width of ≈0.2 eV (unpublished results). While we assume this distribution in the following analysis, it turns out that the final results are rather independent of the detailed shape of $f_0(E_i)$, as was shown by repeating the analysis with the empirical $k_{IR}(E)$ rate changed by ±50%, which is well within the modification applied to the statistical rate coefficient, or even by assuming a Boltzmann distribution for $f_0(E_i)$ with T = 350 K.

For such narrow $f_0(E_i)$ distributions, the integrand $r_\lambda(E, t)$ of the integral in eq 4 is found to be strongly peaked around an average energy $\hat{E}_\lambda(t)$ given by

$$\hat{E}_\lambda(t) = \int_{EA}^{\infty} E r_\lambda(E, t)\, dE / \int_{EA}^{\infty} r_\lambda(E, t)\, dE \tag{5}$$

with $\hat{E}_\lambda(t)$ being almost independent of t. This allows one to approximate eq 4 for $t \geq t_0$ by

$$R(t) \propto k_{VAD}(\hat{E}_\lambda(t_0)) e^{-k_{tot}(\hat{E}_\lambda(t_0))t} \tag{6}$$

which results in an exponential decrease of $R(t)$ with time as approximately observed in the present experiments for $t \geq t_0$ = 16.5 μs, with $k_{tot}(\hat{E}_\lambda(t_0)) = k_\lambda$.

We applied eq 5 to determine $k_{tot}(E)$ from the measured k_λ in an iterative procedure. First we used the rate coefficients measured by Zhao et al.[23] for excitation energies $E_{ph} \gtrsim 5$ eV, where $k_{tot}(E)$ is dominated by $k_{VAD}(E)$, to determine the scaling factor F_{VAD}. No iteration is required in this case; under the conditions of their experiment (initial temperature ≈100 K, $t_0 \gtrsim 50$ ns) $\hat{E}_\lambda(t_0)$ is only slightly larger (≈ 18 meV) than the total absorbed photon energy and found to be independent of $k_{VAD}(E)$. Plotting their data as a function of $\hat{E}_\lambda(t_0)$ and adjusting eq 1 to the data points yield $F_{VAD} = (4.3 \pm 0.9) \times 10^{14}$ s^{-1} (see Figure 3). Next we calculated $\hat{E}_\lambda(t_0)$ for the present measurements. In a first step, the theoretical Einstein coefficients A_j^{th} were used to include the RF contribution to $k_{tot}(E)$. The Einstein coefficients A_j were then adjusted by multiplying the theoretical A_j^{th} with a common scaling factor f_{RF} such that the calculated $k_{tot}(\hat{E}_\lambda(t_0))$ reproduced the measured decay constants, and in a second iteration step the calculation of $\hat{E}_\lambda(t_0)$ and adjustment of the Einstein coefficients was repeated. As the influence of the RF on the determination of $\hat{E}_\lambda(t_0)$ is small, higher iterations were not required. The final result is shown in Figure 3 and leads to a scaling factor of f_{RF} = 1.67 ± 0.33. The error band of $k_{tot}(E)$, resulting from the 20% uncertainty of f_{RF} and F_{VAD}, also encloses the results obtained by allowing for changes of $f_0(E_i)$, as discussed above. As a further check of the consistency of the adopted $f_0(E_i)$ with the data, eq 4 was used together with the deduced $k_{tot}(E)$ to fit the measured $R(t)$ curves, adjusting only the normalization N. As shown by the solid lines in Figure 2, the data are indeed well described.

The good agreement between the decay rate constants observed after one- or two-photon absorption, which involve different excitation paths, nicely corroborates that the C_6^- anions contributing to these decays have undergone intramolecular redistribution over all degrees of freedom. Moreover, the different energy dependence of $k_{tot}(E)$ below ≈4.6 eV from that expected for VAD clearly indicates that a different process starts to dominate the decay in this energy region. While the observed energy dependence of $k_{tot}(E)$ below 4.6 eV would be consistent with the dependence expected for radiative decays via IR transitions, the absolute size is about a factor of 100 too large to be accounted for by infrared transitions. In contrast, scaling the calculated electronic Einstein coefficients A_j by a factor of 1.65 (surprisingly small in view of the contradictory theoretical predictions for the A_j coefficients), the RF process accounts very well for the observed decay rate coefficients. Unfortunately, our data does not allow us to distinguish between the contributions of two electronic states as shown by the thin curves in Figure 3. Allowing the slope to vary within these two extreme assumptions, our experimental result for $k_{RF}(E)$ can be parametrized for around 4.45 eV by

$$k_{RF}(E) = k_{RF}(E_0) e^{\gamma(E-E_0)/E_0} \tag{7}$$

with E_0 = 4.45 eV, $k_{RF}(E_0) = (5.0 \pm 1.0) \times 10^4$ s^{-1}, and $\gamma = (5.1 \pm 2.0)$. Extrapolating to E = EA we find $k_{RF}(EA) \approx 3.7 \times 10^4$ s^{-1}, close to the theoretical estimate of Terzieva and Herbst[12] of 2.8×10^4 s^{-1}. Note that the energy depencence of $k_{RF}(E)$ is observed to be rather weak over the energy range of $(EA - E_0) \approx -0.3$ eV. This leads not only to the exponential time dependence of the decay curves, it also implies that the extracted absolute values for $k_{RF}(E)$ in this energy region are rather independent of the statistical model assumptions used to determine the average total excitation energies $\hat{E}_\lambda$.

In summary, we present the first quantitative measurement of recurrent fluorescence rate coefficients in a small polyatomic molecule. Our result can serve as a benchmark for the validity and accuracy of the statistical approach in describing this process even in light molecules, a process indispensable for understanding the formation and abundance of anions in the interstellar medium: For C_6^- and similar open shell clusters, the RF-mediated radiative rate coefficients are one of the two decisive ingredients to understand their formation from their neutral precursors by radiative electron attachment, the other ingredient being the electron attachment cross section, which can be extracted from VAD rate coefficients by detailed balance. A more precise determination of VAD rate coefficients for C_6^- in the relevant energy region is in progress.

AUTHOR INFORMATION

Corresponding Author

*E-mail: vijayanand.chandrasekaran@weizmann.ac.il.

Notes

The authors declare no competing financial interest.

ACKNOWLEDGMENTS

This research was supported by the Israel Science Foundation (Grant No. 1242/09), by a Yeda Sela Grant, and by a Weizmann Institute Senior Grant. D.S. acknowledges support by the Weizmann Institute of Science through the Joseph Meyerhoff program.

REFERENCES

(1) Bernstein, L. S.; Lynch, D. K. Small Carbonaceous Molecules, Ethylene Oxide (c-C_2H_4O) and Cyclopropenylidene (c-C_3H_2): Sources of the Unidentified Infrared Bands? *Astrophys. J.* **2009**, *704*, 226−239.

(2) Bixon, M.; Jortner, J. Intramolecular Radiationless Transitions. *J. Chem. Phys.* **1968**, *48*, 715−725.

(3) Legér, A.; Boissel, P.; d'Hendecort, L. Predicted Fluorescence Mechanism in Highly Isolated Molecules: The Poincare Fluorescence. *Phys. Rev. Lett.* **1988**, *60*, 921−924.
(4) C. L. Adams, C. L.; Schneider, H.; Weber, J. M. Vibrational Autodetachment - Intramolecular Vibrational Relaxation Translated into Electronic Motion. *J. Phys. Chem. A* **2010**, *114*, 4017−4030.
(5) Karny, Z.; Gupta, A.; Zare, R. N.; Lin, S. T.; Nieman, J.; Ronn, A. M. Collisionless Infrared Multiphoton Production of Electronically Excited Parent Molecules. *Chem. Phys. Lett.* **1979**, *37*, 15−20.
(6) Nitzan, A.; Jortner, A. Inverse Electronic Relaxation. *Chem. Phys. Lett.* **1978**, *60*, 1−4. Nitzan, A.; Jortner, A. Theory of Inverse Electronic Relaxation. *J. Chem. Phys.* **1979**, *71*, 3524−3532.
(7) Borisevich, N. A.; Zalesskaya, G. A.; Urabanovich, A. E. Delayed Luminescence Induced by Multiple Photon Excitation of Ground Electronic State Polyatomic Molecules with CO_2 Laser. *Spectrosc. Lett.* **1990**, *23*, 405−424 and references therein..
(8) Martin, S.; Bernard, J.; Brédy, R.; Concina, B.; Joblin, C.; Ji, M.; Ortega, C.; Chen, L. Fast Radiative Cooling of Anthracene Observed in a Compact Electrostatic Storage Ring. *Phys. Rev. Lett.* **2013**, *110*, 063003−4.
(9) Bernard, J.; Montagne, G.; Brédy, R.; Terpend-Ordacière, B.; Bourgey, A.; Kerleroux, A.; Chen, L.; Schmidt, H. T.; Cederquist, H.; Martin, S. A "Tabletop" Electrostatic Ion Storage Ring: Mini-Ring. *Rev. Sci. Instrum.* **2008**, *79*, 075109−8.
(10) Ito, G.; Furukawa, T.; Tanuma, H.; Matsumoto, J.; Shiromaru, H.; Majima, T.; Goto, M.; Azuma, T.; Hansen, K. Cooling Dynamics of Photoexcited C_6^- and C_6H^-. *Phys. Rev. Lett.* **2014**, *112*, 183001−5.
(11) Jinno, S.; Takao, T.; Hanada, K.; Goto, M.; Okuno, K.; Tanuma, H.; Azuma, T.; Shiromaru, H. Storage and Mass-Selective Control of Ionsin an Electrostatic Ion Storage Ring. *Nucl. Instrum. Methods Phys. Res., Sect. A* **2007**, *572*, 568−579.
(12) Terzieva, R.; Herbst, E. Radiative Electron Attachment to Small Linear Carbon Clusters and Its Significance for the Chemistry of Diffuse Interstellar Clouds. *Int. J. Mass Spectrom.* **2000**, *201*, 135−142.
(13) Aviv, O.; Toker, Y.; Errit, M.; Bhushan, K. G.; Pedersen, H. B.; Rappaport, M. L.; Heber, O.; Schwalm, D.; Zajfman, D. A Bent Electrostatic Ion Beam Trap for Simultaneous Measurements of Fragmentation and Ionization of Cluster Ions. *Rev. Sci. Instrum.* **2008**, *79*, 083110−8.
(14) Arnold, D. W.; Bradforth, S. E.; Kitsopoulos, T. N.; Neumark, D. M. Vibrationally Resolved Spectra of C_2−C_{11} by Anion Photoelectron Spectroscopy. *J. Chem. Phys.* **1991**, *95*, 8753−8764.
(15) Schmatz, S.; Botschwina, P. A Theoretical Investigation of Four Electronic States of C_6^- and the Ground State of Linear C_6. *Chem. Phys. Lett.* **1995**, *235*, 5−12.
(16) Forney, D.; Fulara, J.; Freivogal, P.; Jakobi, M.; Lessen, D.; Maier, J. P. Electronic Absorption Spectra of Linear Carbon Chains in Neon Matrices. I. C_6^-, C_6, and C_6H. *J. Chem. Phys.* **1995**, *103*, 48−53.
(17) Freivogel, P.; Grutter, M.; Forney, D.; Maier, J. P. Electronic Absorption Spectra of C_4^- and C_6^- Chains in Neon Matrices. *J. Chem. Phys.* **1997**, *107*, 22−27.
(18) Cao, Z.; Peyerimhoff, S. D. MRD-CI Characterization of Electronic Spectra of Isoelectronic Species C_6^-, NC_4N^+ and CNC_3N^+. *J. Phys. Chem. A* **2001**, *105*, 627−631.
(19) Gou, X.-G.; Zhang, J.-L.; Zhao, Y. Ab initio Characterization of Size Dependence of Electronic Spectra for Linear Anionic Carbon Clusters C_n^- (n = 4−17). *J. Comput. Chem.* **2011**, *33*, 93−102.
(20) Szczepanski, J.; Ekern, S.; Vala, M. Vibrational Spectroscopy of Small Matrix-Isolated Linear Carbon Cluster Anions. *J. Phys. Chem. A* **1997**, *101*, 1841−1847.
(21) Szczepanski, J.; Auerbach, E.; Vala, M. C_6^- Carbon Cluster Anion: An Infrared Absorption and Resonance Raman Isotopic Study. *J. Phys. Chem. A* **1997**, *101*, 9296−9301.
(22) Fura, A.; Tureček, F.; McLafferty, F. W. Small Carbon Clusters (C_n^0, C_n^+, C_n^-) from Acyclic and Cyclic Precursors: Neutralization−Reionization and Theory. *Int. J. Mass Spec.* **2002**, *217*, 81−96.
(23) Zhao, Y.; Beer, E.; Xu, C.; Taylor, T.; Neumark, D. M. Spectroscopy and Electron Detachment Dynamics of C_4^-, C_6^-, and C_8^-. *J. Chem. Phys.* **1996**, *105*, 4905−4919.
(24) Frischkorn, C.; Bragg, A. E.; Davis, A. V.; Wester, R.; Neumark, D. M. Electronic relaxation dynamics of carbon cluster anions: Excitation of the $\tilde{C}^2\Pi_g \leftarrow \tilde{X}^2\Pi_u$ transition in C_6^-. *J. Chem. Phys.* **2001**, *115*, 11185−11192.
(25) Bragg, A. E.; Verlet, J. R. R.; Kammrath, A.; Neumark, D. M. C_6^- Electronic Relaxation Dynamics Probed via Time-Resolved Photoelectron Imaging. *J. Chem. Phys.* **2004**, *121*, 3515−3526.
(26) Baer, T.; Hase, W. L. *Unimolecular Reaction Dynamics, Theory and Experiments*; Oxford University Press: New York/Oxford, 1996.
(27) Kasperovich, V.; Tikhonov, G.; Kresin, V. V. Low-Energy Electron Capture by free C_{60} and the Importance of Polarization Interaction. *Chem. Phys. Lett.* **2001**, *337*, 55−60.
(28) Whitten, G. Z.; Rabinovitch, B. S. Accurate and Facile Approximation for Vibrational Energy-Level Sums. *J. Chem. Phys.* **1963**, *38*, 2466−2473.
(29) Kurtz, J.; Adamowicz, L. Theoretical Vibrations of Carbon Clusters C_3, C_4, C_5, C_6, C_7, C_8, and C_9. *Astrophys. J.* **1991**, *370*, 784−790.
(30) Boissel, P.; de Parseval, P.; Marty, P.; Lefèvre, G. Fragmentation of Isolated Ions by Multiple Photon Absorption: A Quantitative Study. *J. Chem. Phys.* **1997**, *106*, 4973−4984.
(31) Menk, S. Ph.D Thesis, University of Heidelberg, 2013.http://archiv.ub.uni-heidelberg.de/volltextserver/14912/1/Dissertation_Sebastian_Menk.pdf.